ChemComm

COMMUNICATION

View Article Online
View Journal

Cite this: DOI: 10.1039/d3cc00387f

Received 28th January 2023,
Accepted 18th April 2023

DOI: 10.1039/d3cc00387f

rsc.li/chemcomm

Regulating the Pt_1–CeO_2 interaction *via* alkali modification for boosting the catalytic performance of single-atom catalysts†

Peng Yang,[a] Juntian Xu,[a] Wei Tan,[a] Qinglong Liu,[a] Yandi Cai,[a] Shaohua Xie,[b] Song Hong,[c] Fei Gao,*[a] Fudong Liu[b] and Lin Dong[a]

With the introduction of potassium species, the catalytic oxidation performance over the Pt_1/CeO_2 catalyst was significantly enhanced, where potassium ions acted as structural and electronic promoters, and formed Pt–O–K interactions with Pt to directly regulate the coordination environment and electronic state of Pt and the metal-support interaction between Pt and CeO_2.

With the growth of vehicle ownership, environmental problems caused by vehicle emissions (CO, NO_x, hydrocarbons, *etc.*) have become increasingly serious. Thus, many efforts have been devoted to the emission control field. Among these mitigation strategies, catalytic elimination of vehicle exhaust has been taken as the most promising one. Platinum group metals (PGMs) supported on various metal oxides, such as CeO_2, Al_2O_3, *etc.*, have been extensively applied in emission control systems.

Due to the relatively lower price of Pt compared to Rh and Pd, as well as the promising catalytic oxidation performance of Pt/CeO_2 catalysts, Pt catalysts supported on CeO_2-based materials have attracted the attention of researchers.[1–3] There have been vigorous discussions on Pt single-atom catalysts (SACs) supported on CeO_2 (Pt_1/CeO_2) stemming from the attractive 100% Pt atom utilization and excellent thermal stability. However, the Pt SACs strongly anchored by CeO_2 without further activation treatment always exhibited limited CO oxidation activity,[4,5] while after appropriate activation treatment (*e.g.*, steam aging, CO/H_2/HC reduction), the catalytic oxidation performance of Pt_1/CeO_2 could be substantially promoted.[1,6] Nevertheless, these strict pre-treatment conditions and the relatively high cost of use limited their wide application. Developing a more facile strategy for enhancing the catalytic oxidation activity of Pt_1/CeO_2 is urgently needed. In previous studies, regulating the oxidation state and coordination environment of PGM catalysts as well as tuning the PGM-support interface by introducing other metal oxides or chemical groups to improve their catalytic performance in various reactions has also received extensive concern.[7,8] In many cases, alkali metals (K, Na, Li, *etc.*) have been reported to be effective promoters for some PGM catalysts for various reactions.[9–11] Based on these achievements, there is a promising prospect that alkali modification could be a practical method to improve the catalytic oxidation activity of Pt_1/CeO_2.

Herein, a facile alkali metal (taking K^+ as a representative) modification strategy to promote the catalytic oxidation activity of Pt_1/CeO_2 was proposed by co-depositing potassium and platinum on CeO_2 *via* incipient wetness impregnation. According to the measurements of various characterizations, a clear structure-activity relationship was well established. The deposition of potassium made a difference to Pt_1/CeO_2, which weakened the interaction between Pt and CeO_2 and effectively tuned the oxidation state as well as the coordination environment of Pt sites on Pt_1/CeO_2, which then collectively contributed to the enhancement of its CO/C_3H_8 oxidation activity.

The CO oxidation performances of CeO_2, Pt/CeO_2 and K-Pt/CeO_2 were first evaluated and illustrated in Fig. 1(a) and Table S1 (ESI†). Pt/CeO_2 showed limited CO oxidation activity, which was almost the same as that of pure CeO_2 due to the structural transformation caused by the excessive temperature.[7] After K-modification, the CO oxidation activity on Pt/CeO_2 was dramatically improved, with the T_{50} (temperature at 50% conversion) decreasing from 385 °C to 228 °C and better cycling stability compared to the reduction-activated Pt/CeO_2 (Fig. S1, ESI†). In C_3H_8 oxidation reaction, K-Pt/CeO_2 still performed much better than Pt/CeO_2, further supporting the view that

[a] State Key Laboratory of Pollution Control and Resource Reuse, School of Environment; Jiangsu Key Laboratory of Vehicle Emissions Control, Center of Modern Analysis; Key Laboratory of Mesoscopic Chemistry of MOE, School of Chemistry and Chemical Engineering, Nanjing University, Nanjing 210023, China. E-mail: gaofei@nju.edu.cn

[b] Department of Civil, Environmental, and Construction Engineering, Catalysis Cluster for Renewable Energy and Chemical Transformations (REACT), NanoScience Technology Center (NSTC), University of Central Florida, Orlando, FL 32816, USA

[c] College of Materials Science and Engineering, Beijing University of Chemical Technology, Beijing 100029, China

† Electronic supplementary information (ESI) available. See DOI: https://doi.org/10.1039/d3cc00387f

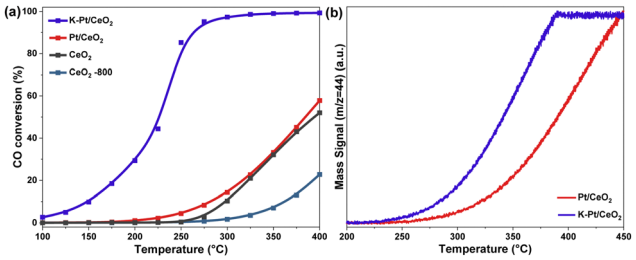

Fig. 1 (a) CO oxidation activities of Pt/CeO_2, K-Pt/CeO_2, CeO_2 and CeO_2 −800. (Reaction atmosphere: 1% CO + 1% O_2, He balanced, and WHSV = 150,000 mL g_{cat}^{-1} h^{-1}.) (b) C_3H_8 oxidation performance of Pt/CeO_2 and K-Pt/CeO_2. (Reaction atmosphere: 4000 ppm propane, 4% O_2/Ar balanced, and WHSV= 100 000 mL g_{cat}^{-1} h^{-1}).

K-modification could promote the catalytic oxidation activity of Pt/CeO_2 catalysts (Fig. 1(b)). Such a significant improvement in the catalytic performance on Pt/CeO_2 after K-modification indicated that the introduction of K^+ might have greatly changed the state of Pt sites on Pt/CeO_2.

According to the results of XRD (Fig. S2, ESI†), for both Pt/CeO_2 and K-Pt/CeO_2 catalysts, only those XRD peaks assigned to CeO_2 (PDF #34-0394) were found, meaning that Pt species in Pt/CeO_2 and K-Pt/CeO_2 were in a highly dispersed state.[12] As demonstrated by the energy-dispersive X-ray spectroscopy and corresponding mapping (EDS-mapping) images of Pt/CeO_2 and K-Pt/CeO_2 (Fig. S3, ESI†), both Pt and K were highly dispersed. To investigate the state of Pt species on Pt/CeO_2 and K-Pt/CeO_2, HAADF-STEM images of these two samples were also collected. As expected, no Pt clusters/particles formed on Pt/CeO_2 and K-Pt/CeO_2. The bright dots marked by yellow circles on Pt/CeO_2 and K-Pt/CeO_2 further indicated that Pt species were mainly in the form of single atoms (Fig. 2(c) and (d)). It has been proven that *in situ* DRIFTS of CO adsorption is a powerful means to probe the state of Pt species on catalysts.[5,13] As shown in Fig. 3(c), only a well-defined band at *ca.* 2090 cm^{-1} was observed on Pt/CeO_2 and K-Pt/CeO_2, which could be assigned to CO adsorbed on ionic Pt single sites (CO-$Pt^{\delta+}$@Pt_1). Maurer *et al.* reported that Pt reconstruction and redispersion can occur during CO oxidation.[4] To clarify whether the Pt species on used Pt/CeO_2 and K-Pt/CeO_2 still existed as single atoms, *in situ* DRIFTS of CO adsorption on used samples were also carried out. Interestingly, after being exposed to CO oxidation reaction flow at 400 °C for 30 min, the bands of CO adsorbed on Pt sites still could be assigned to CO-$Pt^{\delta+}$@Pt_1 species only, implying that Pt species on Pt/CeO_2 and K-Pt/CeO_2 exhibited superior stability and were kept in the single-atom form throughout the reaction, which matched well with the cycling stability results in Fig. S1 (ESI†).

To further investigate the chemical state and coordination environment of Pt species on Pt/CeO_2 and K-Pt/CeO_2, XAS analysis was performed. As shown in Fig. 3(a), the white line intensities of Pt-L_3 XANES for Pt/CeO_2 and K-Pt/CeO_2 were between those for PtO_2 and Pt foil, suggesting an intermediate valence state (between +4 and 0) of Pt on both samples. Besides, EXAFS data were processed and plotted in R space (Fig. 3(b) and Table S2, ESI†), and the absence of Pt–Pt and Pt–O–Pt coordination shells and the existence of Pt–O and Pt–O–Ce coordination shells exclusively clearly confirmed the formation of Pt single sites on Pt/CeO_2 and K-Pt/CeO_2. As shown in Table S2 (ESI†) summarizing the EXAFS Pt L3-edge fitting results, although the coordination number (CN) of Pt–O did not change significantly on Pt/CeO_2 (*ca.* 6.5) *versus* K-Pt/CeO_2 (*ca.* 6.3), a lower CN of Pt–O–Ce was observed on K-Pt/CeO_2

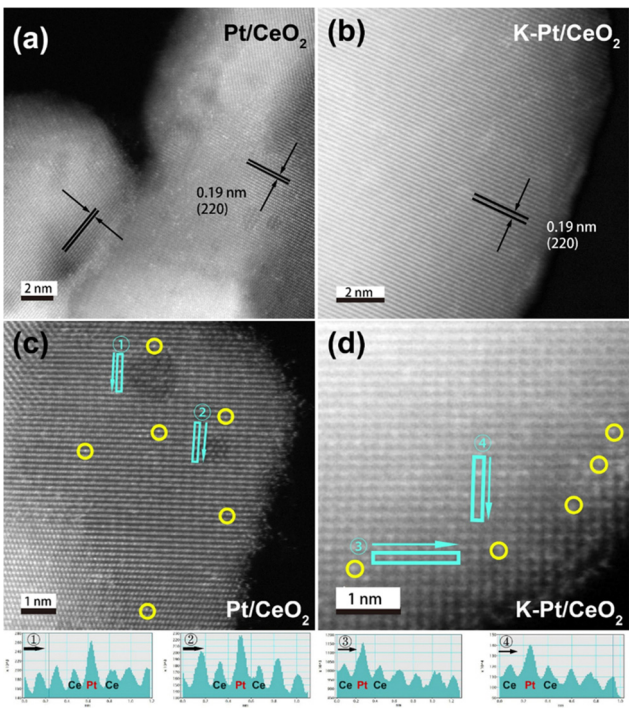

Fig. 2 HAADF-STEM images of (a) and (c) Pt/CeO_2, and (b) and (d) K-Pt/CeO_2. (Some of the single atomic Pt sites were identified by yellow circles.)

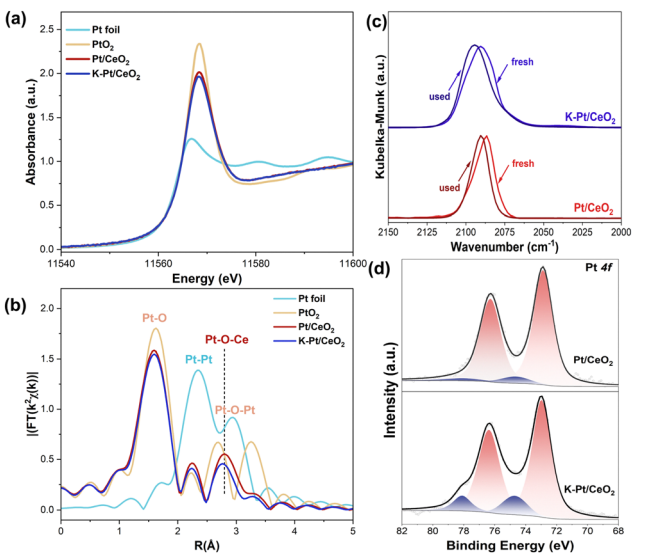

Fig. 3 (a) XANES and (b) EXAFS data recorded at the Pt L_3 edge for Pt/CeO_2 and K-Pt/CeO_2. (c) *In situ* DRIFTS of CO adsorption on fresh and used Pt/CeO_2 and K-Pt/CeO_2. (d) Pt 4f XPS spectra of Pt/CeO_2 and K-Pt/CeO_2.

(*ca.* 2.9) than that on Pt/CeO_2 (*ca.* 4.0), suggesting that K-modification has tuned the coordination environment of Pt atoms and the interaction between Pt and the CeO_2 support. It was proposed that Pt–O–Ce linkages may have been broken and Pt–O–K linkages were formed simultaneously, which can be further clarified by the ICP results shown in Table S3 (ESI†), where the Pt/K ratio was close to 1 : 1 for different loadings, while K cannot be retained on the CeO_2 surface in the absence of Pt when calcined at a high temperature of 800 °C.

Since the Pt species on Pt/CeO_2 and $K\text{-}Pt/CeO_2$ were both in the form of single atoms, it could be inferred that the electronic state of Pt or the interaction between Pt and the CeO_2 support must be tuned by K-modification. To accurately characterize the chemical state of the surface Pt species, XPS was performed on Pt/CeO_2 and $K\text{-}Pt/CeO_2$. As shown in Fig. 3(d), for Pt/CeO_2, Pt species mainly existed in the form of Pt^{2+} (93%), well supported by the previous reports that Pt single atoms strongly anchored on CeO_2 with a valence state of +2.[1,14] It was interesting to find that a higher ratio of Pt^{4+} (14.6%) formed on $K\text{-}Pt/CeO_2$, which confirmed that K^+ could perform as an electronic promoter. In previous research,[15] it has been found that ionic Pt single atoms with higher valence always exhibited higher CO oxidation activity. Zhang *et al.* also reported that $Pt^{\delta+}$ with higher valence can induce C–H dissociation more easily.[16] According to the fitting results of Ce 3d and O 1s XPS (Fig. S4, S5 and Table S4, ESI†), no obvious changes in the concentration of surface Ce^{4+} and the ratio of surface chemisorbed oxygen species were observed after the potassium modification, suggesting that the changed state of Pt species dominated the significant improvement in the catalytic performance of $K\text{-}Pt/CeO_2$.

H_2-temperature programmed reduction (H_2-TPR) could be applied not only to investigate the redox properties of the catalysts but also to dig out the structural information of samples. As shown in Fig. 4(a), the H_2 consumption peaks at *ca.* 370 and 530 °C on CeO_2 could be assigned to the reduction of surface oxygen species and Ce^{4+} and the H_2 consumption occurring at higher temperatures should be related to the reduction of bulk CeO_2. For Pt/CeO_2, an intensive H_2 consumption peak assigned to the reduction of Pt–O–Ce and adjacent Ce^{4+} species was observed at *ca.* 260 °C. Interestingly, after K-modification, the H_2 consumption peak of Pt–O–Ce shifted to a much lower temperature of 164 °C with a decreased intensity, which meant that the strong interaction between Pt single sites and CeO_2 was weakened by potassium. The lower temperature required for the reduction of Pt species on $K\text{-}Pt/CeO_2$ could facilitate the activation of reactants in the low temperature range. That is, those Pt single sites on the CeO_2 support with over-strong Pt–O–Ce interactions were not efficient in CO oxidation reaction.

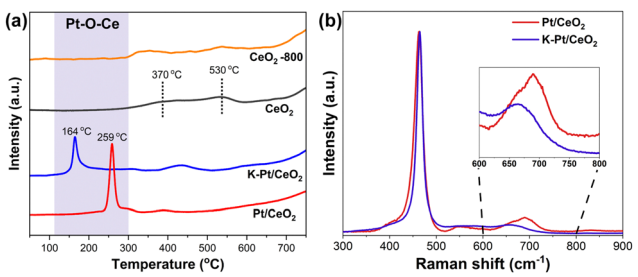

Fig. 4 (a) H_2-TPR profiles of Pt/CeO_2, $K\text{-}Pt/CeO_2$, CeO_2 and CeO_2-800. (b) Raman spectroscopy of Pt/CeO_2 and $K\text{-}Pt/CeO_2$ with the scale at 300–900 cm^{-1}.

As reported previously, Raman spectroscopy could be used as a powerful tool to investigate the structure of $Pt\text{–}CeO_2$-based catalysts. As illustrated in Fig. 4(b), in addition to the intensive band at *ca.* 460 cm^{-1} and the broad band at *ca.* 600 cm^{-1}, which could be ascribed to the F_{2g} vibration mode of CeO_2[17] and $V_O\text{–}Ce^{3+}$ induced by oxygen vacancies on CeO_2,[18] respectively, two new bands at *ca.* 550 and 670 cm^{-1} emerged on Pt/CeO_2 and $K\text{-}Pt/CeO_2$, which were related to the formation of Pt–O–Ce linkages. Consistent with the H_2-TPR results, as demonstrated by the inset figure, the intensity of the bands at *ca.* 670 cm^{-1} (Pt–O–Ce) decreased dramatically after K-modification, implying that potassium modification could weaken the $Pt\text{–}CeO_2$ interaction and reduced the amount of Pt–O–Ce linkages. The lower CN of Pt–O–Ce on $K\text{-}Pt/CeO_2$ (*ca.* 2.9) than that on Pt/CeO_2 (*ca.* 4.0) from EXAFS data also indicated that less Pt–O–Ce linkages were formed on $K\text{-}Pt/CeO_2$, supporting the Raman spectroscopy and H_2-TPR results (Table S2, ESI†).

Furthermore, it has been reported that the deposition of Pt could stabilize CeO_2 through the strong $Pt\text{–}CeO_2$ interaction under high-temperature aging treatment.[14] That is why Pt/CeO_2 possessed a much higher specific surface area (32 $m^2\ g^{-1}$) than CeO_2 -800 (CeO_2 calcined at 800 °C in air for 10 h, 6.5 $m^2\ g^{-1}$). However, it was noteworthy that $K\text{-}Pt/CeO_2$ showed a much lower specific surface area (11 $m^2\ g^{-1}$) compared with Pt/CeO_2 (Table S1, ESI†), hinting at the weakened $Pt\text{-}CeO_2$ interaction on $K\text{-}Pt/CeO_2$, which resulted in the more intensive sintering of CeO_2.

As discussed above, the catalytic oxidation performance of Pt/CeO_2 and $K\text{-}Pt/CeO_2$ was strongly related to the strength of $Pt\text{–}CeO_2$ interaction, as well as the amount of Pt–O–Ce linkages. In order to better reveal the reasons for the dramatic improvement of the alkali modification on the catalytic oxidation performance of Pt/CeO_2 and establish a clear structure–activity relationship, the results of the catalytic performance evaluation, XPS, Raman spectroscopy, H_2-TPR and CN of Pt–O–Ce were rearranged and are demonstrated in Fig. 5. After K-modification, an increase in the valence state of Pt suggested that K ions might be located near the Pt single sites and they acted as an electronic promoter modifying the electronic state of the nearby Pt sites. The weakened $Pt\text{–}CeO_2$ interaction was well supported by the remarkable shift of the H_2 consumption peak of Pt–O–Ce species from 259 to 164 °C. In addition, the H_2 consumption of Pt–O–Ce decreased with the potassium modification and the peak area of Pt–O–Ce species (*ca.* 670 cm^{-1}) in Raman spectroscopy and the coordination number of Pt–O–Ce also decreased, further demonstrating the breakage of partial Pt–O–Ce linkages. In this study, Pt/CeO_2 was subjected to a calcination treatment at 800 °C for 10 h during the catalyst synthesis, and thus Pt atoms were captured by the CeO_2 support through over-strong Pt–O–Ce linkages. The oxidation of adsorbed CO on Pt single sites required the activation of adjacent oxygen species. However, as demonstrated in Fig. 5, the

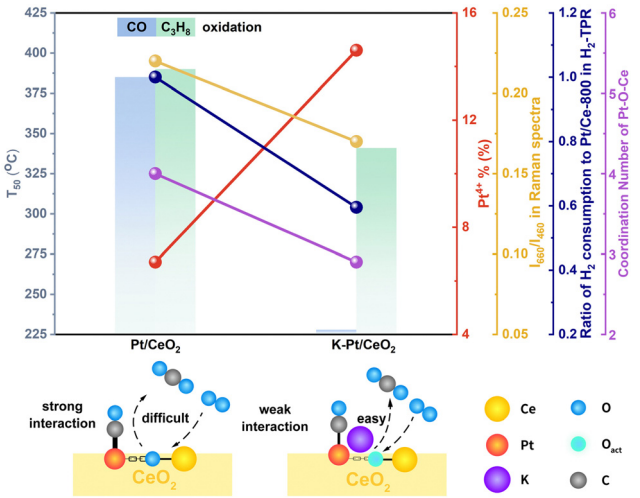

Fig. 5 The structure–activity relationship and the process of CO oxidation on Pt/CeO_2 and K-Pt/CeO_2.

rigid Pt–O–Ce interaction inhibited the activation and mobility of surface oxygen atoms. That's why Pt/CeO_2 exhibited a rather limited CO oxidation activity, just like pure CeO_2. *Via* introducing K ions, the Pt–CeO_2 interaction on Pt/CeO_2 was appropriately weakened so that the reducibility of Pt–O–Ce in K-Pt/CeO_2 was greatly improved. In other words, oxygen species at the interface of Pt and the CeO_2 support could react more efficiently with CO adsorbed on Pt single sites, thus improving the catalytic oxidation capability of K-Pt/CeO_2, which could be illustrated by the O_2-TPD profiles in Fig. S6 (ESI†).

In conclusion, Pt_1/CeO_2 with over-strong Pt-CeO_2 interaction was not an efficient catalyst in CO/hydrocarbon oxidation reaction. *Via* a simple potassium modification method, the catalytic oxidation performance of Pt_1/CeO_2 was significantly promoted. It was found that the introduction of K ions weakened the Pt–CeO_2 interaction appropriately and formed Pt–O–K interaction, which could improve the reducibility of the Pt–O–Ce structure. Then the activation of oxygen atoms adjacent to Pt single sites and their subsequent reaction with adsorbed CO would be facilitated. As a result, superior catalytic oxidation performance was achieved on K-Pt/CeO_2. This work highlighted that alkali could be used as an electronic and structural promoter to finely tune the state of PGMs and the strength of PGM-support interaction, and provided a simple but effective strategy for the design of efficient vehicle emission control catalysts.

Peng Yang: data curation, formal analysis, and writing – original draft; Juntian Xu: investigation, validation, and visualization; Wei Tan: conceptualization, methodology; Qinglong Liu: validation; Yandi Cai: resources; Shaohua Xie: resources, visualization; Song Hong: software, resources; Fei Gao: conceptualization, funding acquisition, and supervision; Fudong Liu: resources, writing – review and editing; and Lin Dong: supervision.

This work was supported by the National Natural Science Foundation of China (No. 21972063) and the Natural Science Foundation of Jiangsu Province (BK20200012). This research used beamline 7-BM (QAS) of the National Synchrotron Light Source II (NSLS-II), a U.S. Department of Energy (DOE) Office of Science User Facility operated for the DOE Office of Science by Brookhaven National Laboratory (BNL) under Contract No. DE-SC0012704. F. Liu sincerely thanks Dr Lu Ma and Dr Steven N. Ehrlich at 7-BM (QAS), NSLS-II, BNL for help with XAS measurements.

Conflicts of interest

There are no conflicts to declare.

Notes and references

1 X. I. Pereira-Hernández, A. DeLaRiva, V. Muravev, D. Kunwar, H. Xiong, B. Sudduth, M. Engelhard, L. Kovarik, E. J. Hensen, Y. Wang and A. K. Datye, *Nat. Commun.*, 2019, **10**, 1358.
2 L. Chen, P. Verma, K. Hou, Z. Qi, S. Zhang, Y.-S. Liu, J. Guo, V. Stavila, M. D. Allendorf, L. Zheng, M. Salmeron, D. Prendergast, G. A. Somorjai and J. Su, *Nat. Commun.*, 2022, **13**, 1092.
3 T. R. Reina, M. Gonzalez-Castaño, V. Lopez-Flores, L. M. Martínez T, A. Zitolo, S. Ivanova, W. Xu, M. A. Centeno, J. A. Rodriguez and J. A. Odriozola, *J. Am. Chem. Soc.*, 2022, **144**, 446–453.
4 F. Maurer, J. Jelic, J. Wang, A. Gänzler, P. Dolcet, C. Wöll, Y. Wang, F. Studt, M. Casapu and J.-D. Grunwaldt, *Nat. Catal.*, 2020, **3**, 824–833.
5 Y. Lu, S. Zhou, C.-T. Kuo, D. Kunwar, C. Thompson, A. S. Hoffman, A. Boubnov, S. Lin, A. K. Datye, H. Guo and A. M. Karim, *ACS Catal.*, 2021, **11**, 8701–8715.
6 L. A. Avakyan, N. A. Kolpacheva, E. V. Paramonova, J. Singh, U. Hartfelder, J. A. van Bokhoven and L. A. Bugaev, *J. Phys. Chem. C*, 2016, **120**, 28057–28066.
7 W. Tan, S. Xie, D. Le, W. Diao, M. Wang, K.-B. Low, D. Austin, S. Hong, F. Gao, L. Dong, L. Ma, S. N. Ehrlich, T. S. Rahman and F. Liu, *Nat. Commun.*, 2022, **13**, 7070.
8 Y. Ma, B. Chi, W. Liu, L. Cao, Y. Lin, X. Zhang, X. Ye, S. Wei and J. Lu, *ACS Catal.*, 2019, **9**, 8404–8412.
9 R. Qin, L. Zhou, P. Liu, Y. Gong, K. Liu, C. Xu, Y. Zhao, L. Gu, G. Fu and N. Zheng, *Nat. Catal.*, 2020, **3**, 703–709.
10 Y. Zhai, D. Pierre, R. Si, W. Deng, P. Ferrin, A. U. Nilekar, G. Peng, J. A. Herron, D. C. Bell, H. Saltsburg, M. Mavrikakis and M. Flytzani-Stephanopoulos, *Science*, 2010, **329**, 1633–1636.
11 C. Wang, Y. Li, L. Zheng, C. Zhang, Y. Wang, W. Shan, F. Liu and H. He, *ACS Catal.*, 2021, **11**, 456–465.
12 R. Gu, D. Meng, M. She, Y. Wang, H. Yang, X. Guo, N. Xue and W. Ding, *Chem. Commun.*, 2022, **58**, 7630–7633.
13 J. Ke, W. Zhu, Y. Jiang, R. Si, Y.-J. Wang, S.-C. Li, C. Jin, H. Liu, W.-G. Song, C.-H. Yan and Y.-W. Zhang, ACS, *Catalysis*, 2015, **5**, 5164–5173.
14 J. Lee, Y. Ryou, X. Chan, T. J. Kim and D. H. Kim, *J. Phys. Chem. C*, 2016, **120**, 25870–25879.
15 Y. Tang, Y.-G. Wang and J. Liu, *J. Phys. Chem. C*, 2017, **121**, 11281–11289.
16 F. Zhang, R. A. Gutiérrez, P. G. Lustemberg, Z. Liu, N. Rui, T. Wu, P. J. Ramírez, W. Xu, H. Idriss, M. V. Ganduglia-Pirovano, S. D. Senanayake and J. A. Rodriguez, *ACS Catal.*, 2021, **11**, 1613–1623.
17 W. Zou, C. Ge, M. Lu, S. Wu, Y. Wang, J. Sun, Y. Pu, C. Tang, F. Gao and L. Dong, *RSC Adv.*, 2015, **5**, 98335–98343.
18 W. Tan, S. Xie, X. Wang, C. Wang, Y. Li, T. E. Shaw, L. Ma, S. N. Ehrlich, A. Liu, J. Ji, F. Gao, L. Dong and F. Liu, *Chem. Eng. J.*, 2021, **426**, 131855.

